Developmental Biology 455 (2019) 42–50

Contents lists available at ScienceDirect

Developmental Biology

journal homepage: www.elsevier.com/locate/developmentalbiology

DC-SCRIPT deficiency delays mouse mammary gland development and branching morphogenesis

Chunling Tang [a], Renske J.E. van den Bijgaart [a], Maaike W.G. Looman [a], Nina Tel-Karthaus [a], Annemarie M.A. de Graaf [a], Susan Gilfillan [b], Marco Colonna [b], Marleen Ansems [a,**,1], Gosse J. Adema [a,*,1]

[a] Radiotherapy & OncoImmunology Laboratory, Department of Radiation Oncology, Radboud Institute for Molecular Life Sciences, Radboud University Medical Center, 6525 GA, Nijmegen, the Netherlands
[b] Department of Pathology and Immunology, Washington University School of Medicine, St. Louis, MO63110, USA

ARTICLE INFO

Keywords:
DC-SCRIPT/*Zfp366*
Mammary gland morphogenesis
Organoids
3D culture

ABSTRACT

Mammary glands are unique organs in which major adaptive changes occur in morphogenesis and development after birth. Breast cancer is the most common cancer and a major cause of mortality in females worldwide. We have previously identified the loss of expression of the transcription regulator DC-SCRIPT (*Zfp366*) as a prominent prognostic event in estrogen receptor positive breast cancer patients. DC-SCRIPT affects multiple transcriptional events in breast cancer cells, including estrogen and progesterone receptor-mediated transcription, and promotes CDKN2B-related cell cycle arrest. As loss of DC-SCRIPT expression appears an early event in breast cancer development, we here investigated the role of DC-SCRIPT in mammary gland development using wild-type and DC-SCRIPT knockout mice. Mice lacking DC-SCRIPT exhibited severe breeding problems and showed significant growth delay relative to littermate wild-type mice. Subsequent analysis revealed that DC-SCRIPT was expressed in mouse mammary epithelium and that DC-SCRIPT deficiency delayed mammary gland morphogenesis *in vivo*. Finally, analysis of 3D mammary gland organoid cultures confirmed that loss of DC-SCRIPT dramatically delayed mammary organoid branching *in vitro*. The study shows for the first time that DC-SCRIPT deficiency delays mammary gland morphogenesis *in vivo* and *in vitro*. These data define DC-SCRIPT as a novel modulator of mammary gland development.

1. Introduction

The transcription factor dendritic cell specific transcript (DC-SCRIPT or *Zfp366*) was originally identified in dendritic cells (DCs) and shown to be also present in ductal epithelial cells (Triantis et al., 2006a, 2006b; Ansems et al., 2010a). Subsequent studies in epithelial cancers identified loss of DC-SCRIPT expression as a significant prognostic marker in estrogen receptor (ER) positive breast cancer patients (Ansems et al., 2010a; Sieuwerts et al., 2010). In breast tumor cells, DC-SCRIPT acts as a coregulator of multiple type I and type II nuclear receptors (NRs) governing breast cancer cell fate decisions during breast cancer progression (Ansems et al., 2010a; Sieuwerts et al., 2010). Strikingly, DC-SCRIPT displays repressive activity on type I NR-mediated transcription (ER, Progesterone Receptor), while at the same time stimulating the anti-proliferative type II NRs (Peroxisome Proliferator Activated Receptor, Retinoic Acid Receptor) (Ansems et al., 2010a, 2010b, 2012). In line with DC-SCRIPT acting as a breast cancer suppressor, we recently reported that DC-SCRIPT induces cell cycle arrest through promoting CDKN2B expression in ER positive breast cancer cells (Ansems et al., 2015). The presence of DC-SCRIPT in MCF7 breast cancer cell line *via* a

* Corresponding author. Department of Radiotherapy, Radboud University Medical Center, Route 874, Geert Grooteplein-Zuid 32, 6525 GA, Nijmegen, the Netherlands.
** Corresponding author. Department of Radiotherapy, Radboud University Medical Center, Route 874, Geert Grooteplein-Zuid 32, 6525 GA, Nijmegen, the Netherlands.
E-mail addresses: Chunling.Tang@radboudumc.nl (C. Tang), Renske.vandenBijgaart@radboudumc.nl (R.J.E. van den Bijgaart), Maaike.Looman@radboudumc.nl (M.W.G. Looman), Nkarthaus@viecuri.nl (N. Tel-Karthaus), A.M.A.de_Graaf@LUMC.nl (A.M.A. de Graaf), sgilfillan@wustl.edu (S. Gilfillan), mcolonna@wustl.edu (M. Colonna), Marleen.Ansems@radboudumc.nl (M. Ansems), Gosse.Adema@radboudumc.nl (G.J. Adema).
[1] shared last authors.

https://doi.org/10.1016/j.ydbio.2019.06.023
Received 24 January 2019; Received in revised form 28 June 2019; Accepted 28 June 2019
Available online 29 June 2019

doxycycline-induced system not only reduces cell viability *in vitro* but also inhibits tumor growth in an *in vivo* MCF7 cell line derived tumor xenografts model (Ansems et al., 2015). In DCs, DC-SCRIPT was shown to regulate IL-10 expression *via* modulating DUSP4 (Dual Specificity Phosphatase 4) activity, MAPK (Mitogen-activated protein kinases) signaling and activation and binding of NF-κBp65 to the IL10 enhancer (Triantis et al., 2006a; Sondergaard et al., 2015, 2018). In addition, DC-SCRIPT also functions as a corepressor of glucocorticoid receptor-mediated transcription in human monocyte–derived DCs (Hontelez et al., 2013). These data show that DC-SCRIPT can affect both NR-mediated transcriptional processes as well as the MAPK signaling pathway.

The NR-mediated regulatory networks driven by reproductive hormones that are regulated by DC-SCRIPT are also known to be crucial for mammary gland development (Brisken, 2002; Brisken and O'Malley, 2010). Mammary glands are specialized organs responsible for nourishing newborn *via* producing and secretion of milk. Different from most other organs that are patterned during embryonic development, the mammary gland undergoes dramatic morphogenetic changes after birth (Smith, 2012; Macias and Hinck, 2012). Postnatal mammary gland development is tightly regulated during each developmental stage including puberty, pregnancy, lactation, and regression (Brisken and O'Malley, 2010; Hennighausen and Robinson, 2005). Branching morphogenesis is a defined feature during pubertal development and is characterized by the formation of terminal end buds (TEBs) at the distal tip of epithelial ducts. These structures drive extensive mammary ductal tree outgrowth and bifurcation (Ball, 1998; Paine and Lewis, 2017). Once the ductal tree reaches the limit of the fat pad by the end of puberty stage, TEBs are totally regressed and the mammary gland is ready for the next stage (Macias and Hinck, 2012; Ball, 1998). Throughout the female reproductive lifetime, mammary gland adaptations are under continuous control of systemic hormones (*e.g.* estrogen, progesterone) and other factors (Brisken and O'Malley, 2010; Asselin-Labat et al., 2010; Joshi et al., 2010). However, the role of DC-SCRIPT during mammary gland development and tissue homeostasis has not been investigated. This study could contribute to our understanding of the role of DC-SCRIPT in breast cancer tumorigenesis.

We have previously shown that DC-SCRIPT is expressed by ductal epithelial cells in the mammary gland (Ansems et al., 2010a). The ductal tree of a mammary gland is composed of an outer layer of myoepithelium and an inner layer of luminal epithelium. The basal epithelium layer consists mainly of mature contractile myoepithelial cells, but also contains mammary stem cells (MaSCs) (Prater et al., 2014). These multi-potent cells have the capacity to generate both basal and luminal layers (Lloyd-Lewis et al., 2017; Visvader and Stingl, 2014). Recently studies have reported a striking heterogeneity within MaSCs and precise details of cell fate decision need further studies (Trejo et al., 2017; Fu et al., 2017; Wang et al., 2015). Within the luminal compartment, populations of progenitors and functionally differentiated cells can be distinguished by established cell surface markers (Giraddi et al., 2015; Shehata et al., 2012). Differentiated or mature luminal cell subsets, including hormone-sensing ER positive cells, are defined as $Sca1^{+}CD49b^{-}$ cells, while the precursor populations have a $Sca1^{-}CD49b^{+}$ and $Sca1^{+}CD49b^{+}$ phenotype (Giraddi et al., 2015; Shehata et al., 2012).

In this study, the expression of DC-SCRIPT in mouse mammary gland epithelial cells was evaluated as well as its impact on mammary gland morphogenesis. Our results show that DC-SCRIPT is expressed in both basal and luminal epithelium. Studies using littermate wild-type mice and DC-SCRIPT deficient mice revealed that mammary gland morphogenesis was dramatically impaired in the absence of DC-SCRIPT during puberty and early adult stage. Furthermore, DC-SCRIPT deletion delayed mammary gland organoid branching *in vitro* in 3D organoid cultures. Collectively, these findings demonstrate for the first time that DC-SCRIPT plays an important role in controlling mammary gland development.

2. Materials and methods

2.1. Antibodies and reagents

The following primary antibodies were used: CD31-PE (1:80 dilution, Antibodychain, Cat. #1112040), CD31-PE/Cy7 (1:80 dilution, eBioscience, Cat. #25-0311-82), TER119-PE (1:80 dilution, eBioscience, Cat. #12-5921-81), TER119-PerCP (1:80 dilution, Antibodychain, Cat. #1181130), CD45.2-BV510 (1:100 dilution, Antibodychain, Cat. #1149185), CD45.2-PerCP (1:200 dilution, BD, Cat. #552950), CD24-BV510 (1:100 dilution, Biolegend, Cat. #101831), EpCAM-FITC (1:400 dilution, eBioscience, Cat. #11-5791-82), CD49f-APC (1:400 dilution, eBioscience, Cat. #17-0495-80), Sca1-APC/Cy7 (1:100 dilution, Biolegend, Cat. #108125), CD49b-PE/Cy7 (1:50 dilution, eBioscience, Cat. #25-5971-82), Rabbit monoclonal anti-Keratin 8 antibody (1:200 dilution, Abcam, Cat. #ab53280), Rabbit Polyclonal anti-Keratin 14 antibody (1:200 dilution, Biolegend, Cat. #905301). Mouse monoclonal anti-DC-SCRIPT antibody (891ug/ml, 1:90 dilution) were produced in-house. The following isotypes were used: purified Mouse IgG isotype (Biolegend, Cat. #400102), purified Rabbit IgG isotype (Cell Signaling Technology, Cat. #3900S). The following secondary antibodies were used: Alexa fluor 488 conjugated donkey anti-Rabbit IgG (1:400 dilution, Molecular Probes, Cat. #A21206), Cy3 conjugated donkey anti-Mouse IgG (1:100 dilution, Jackson ImmunoResearch, Cat. #715-166-151). The following reagents were purchased and used: Growth Factor Reduced Matrigel (Corning, Cat. #354230), DNAse I (Roche, Cat. #11284932001), TrypLE (Gibco, Cat. #12605–010), DMEM/F12 (Gibco, Cat. #11330057), FGF2 (Sigma, Cat. #F0291-25UG), Collagenase A (Sigma, Cat. #C5138–1F), Insulin-transferrin-selenium-X, (Gibco, Cat. #51500), Antibiotic-Antimycotic (100X) (Gibco, Cat. #15240062), TRIzol reagent (Invitrogen, Cat. #15596026), SYBR Green Master (Roche, Cat. #4673492001), Carmine (Sigma, Cat. #C1022), Aluminum potassium sulfate (Sigma, Cat. #A7167), Histosafe (Adamas Instrumenten B.V.), DNase I (amplification grade, Invitrogen, Cat. #18068015), Hexamers (Invitrogen, Cat. #N8080127), Moloney Murine Leukemia Virus (M-MLV) Reverse Transcriptase (Invitrogen, Cat. #28025013).

2.2. Mice

All mice used were 3–18 weeks old female mice on a C57BL/6 background. DC-SCRIPT knockout mice ($DC\text{-}SCRIPT^{-/-}$) and control littermate wild-type mice ($DC\text{-}SCRIPT^{+/+}$) were bred and housed at the Animal Research Facility of the Radboud University Medical Center. All animal experiments were documented and approved by the Animal Experimental Committee of the Radboud University Medical Center and were performed in accordance with regulatory standards of the Animal Experimental Committee.

2.3. Generation of DC-SCRIPT knockout mice

DC-SCRIPT (*Zfp366*) knockout mice were generated at Washington University by deletion of a 2306bp fragment containing the ATG translation initiation codon and all of exon 2 (Fig. S1A). Briefly, the targeting construct was linearized and electroporated into a B6-albino (B6(Cg)-Tyr^{c-2J}/J) embryonic stem cell line. One clone carrying the correctly modified *Zfp366* locus was identified by Southern blot analysis and PCR, expanded and injected into C57BL/6 blastocysts to produce chimeric mice as previously described (Riegert and Gilfillan, 1999). Chimeras were initially bred to B6-albino mice to easily assess germline transmission; the presence of the targeted *Zfp366* allele was confirmed by PCR analysis. Targeted mice were further intercrossed or bred with transgenic mice expressing the Cre recombinase under control of the CMV promoter (B6.C-Tg(CMV-cre)1Cgn) to generate DC-SCRIPT total knockout mice (Schwenk et al., 1995). For continued maintenance of the line, DC-SCRIPT knockout mice were backcrossed onto a C57BL/6J

background and offspring were identified by PCR genotyping (Fig. S1B). All protocols were carried out in accordance with and approved by the Institutional Animal Care and Use Committee at Washington University in St. Louis, MO.

2.4. Mendelian ratio and growth curve analysis

For Mendelian ratio calculation, heterozygous female DC-SCRIPT mice aged 7–9 weeks were mated with heterozygous male DC-SCRIPT mice. 312 live pups in total were obtained from 25 different parent pairs during one whole year breeding. The genotype of all pups was determined and the percentage of pups with different genotype was calculated. For growth-curve analysis, in total 456 mice with different ages were obtained and body weight was recorded from DC-SCRIPT$^{-/-}$ mice and their littermate controls.

2.5. Mammary whole mount carmine staining and morphological analysis

The right inguinal mammary gland (#4) was excised and whole-mounted on a glass slide. After fixing in Carnoy's solution (75% ethanol, 25% glacial acetic acid) overnight at 4 °C, the mammary gland was rehydrated in ethanol with decreasing concentrations (70%, 50% and 0%) and stained with carmine red overnight at 4 °C. Then the mammary gland was dehydrated progressively in increasing concentrations of ethanol (70%, 95%, and 100%) and cleared in Histosafe for lipid removal. Stained mammary glands were imaged in a tile scan pattern of Leica DMI6000 epi-fluorescence microscope fitted with a 10x objective. Images were analyzed and quantified with Image J software. Briefly, mammary epithelium surface area was quantified as the region occupied by mammary epithelial ducts from the primary stalk to all terminal ends of the branching network. For ductal distance measurement, the ductal length of mammary gland in 7 weeks and 18 weeks old mice was determined by measuring the distance between the center of the lymph node and the end of the longest duct. In 3 weeks old mouse, the ductal length of mammary gland was not measured as the ducts did not yet reach the lymph node. Total branch point number was quantified as the total number of primary, secondary and tertiary branches from the primary stalk of each ductal network. Furthermore, the total number of TEBs was counted in 7 and 8 weeks old mice.

2.6. Immunofluorescence microscopy

Mammary glands sections were prepared for immunofluorescence staining after being dissected from mice. Briefly, mammary glands were fixed in 4% paraformaldehyde overnight at 4 °C and thereafter embedded in paraffin and sectioned (4 μm). For immunofluorescence staining, sections were deparaffinized and rehydrated. After boiling in retrieval solution for 30 min for antigen retrieval, sections were treated with blocking buffer for 30 min at room temperature and were subsequently incubated in primary antibodies overnight at 4 °C, followed by incubation in secondary antibodies for 45 min at 37 °C. Nuclei were stained and visualized using DAPI (4′6-diamidino-2-phenylindole) with incubation at room temperature for 15 min. Images were captured with a Leica DM 6000 microscope using IP-lab imaging software (Scanalytics Inc., Fairfax, VA, USA).

2.7. Mammary gland organoids isolation

Mammary glands (#3, #4 and #5) were freshly dissected from female mice for isolating mammary gland fragments after removing the lymph node as described previously (Nguyen-Ngoc et al., 2015; Plaks et al., 2015). Briefly, mammary glands were minced and digested in 2 μg/ml collagenase A solution (10 ml DMEM/F12, 5 μg/ml insulin, 5% fetal bovine serum, 1% Antibiotic-Antimycotic) for 35 min at 37 °C with shaking at 150 rpm. After digestion, samples were washed with DMEM/F12 and enriched by centrifugation. Then samples were subjected to DNase I (40 U/ml) treatment and followed by differential centrifugation to enrich mammary glands fragments.

2.8. Single cell preparation, flow cytometry analysis and cell sorting

Single-cell suspensions of mammary epithelium were generated from mammary gland fragments by digesting them in TrypLE for 15 min at 37 °C. Single cells were treated with blocking buffer for 10 min at 4 °C and were stained with antibodies as listed above with incubation at 4 °C for 30 min. Subsequent flow cytometry analysis was conducted on a FACS Verse (BD Biosciences) and Fluorescence-activated cell sorting (FACS) was performed on a FACS ARIA III (BD Biosciences). Fixable Viability Dyes (FVD) eFluor™ 450 was added to distinguish dead and live cells. Data were analyzed using FlowJo V10 software (Tree Star).

2.9. 3D mammary gland organoid culture and branching assay

3D mammary gland organoid cultures and branching quantifications were described previously (Nguyen-Ngoc et al., 2015; Plaks et al., 2015). Briefly, mammary gland organoids (50–100) from 18 weeks old female mouse were embedded in 50 μl Growth Factor Reduced Phenol-Red Free Matrigel in 24 wells plates and grown in organoid medium (DMEM/F12, 1% Antibiotic-Antimycotic, 1% Insulin-transferrin-selenium-X and 50 ng/ml FGF2). Medium was refreshed every two days. Branching was quantified on day 4, day 5 and day 6. Briefly, organoids were divided into 4 grades based on branching status: Grade 0, no branches; Grade 1, 1–3 branches; Grade 2, 4–6 branches; Grade 3, more than 6 branches. The percentage of each grade organoid was calculated by dividing the total number of corresponding grade organoids to the total amount of organoids in each well. Organoids from three wells per mouse were quantified per experiment, in total data were collected from 4 mice of each genotype.

2.10. RNA preparation and quantitative RT-PCR

Sorted mammary epithelium or organoids samples were directly lysed in TRIzol Reagent for total RNA extraction. RNA quantity and purity were determined on a NanoDrop 2000/2000c spectrophotometer (Thermo Scientific). After treatment with DNase I, RNA was reverse transcribed into cDNA by using random hexamers and M-MLV reverse transcriptase according to the manufacturer's instructions. Quantitative RT-PCR was performed in a CFX96 sequence detection system (Bio-Rad) with SYBR Green as the fluorophore and gene-specific oligonucleotide primers to determine the mRNA levels for the genes of interest. Reaction mixtures and program conditions were used as recommended by the manufacturer (Bio-Rad). Quantitative PCR data were analyzed with the CFX Manager software (Bio-Rad) as described before (Hontelez et al., 2013), and mRNA levels were calculated according to the cycle threshold method (Livak and Schmittgen, 2001). The primers (from forward to reverse) for mouse genes were listed below:

DC-SCRIPT (Zfp366): ACCAGTGTCATCTCTGCTAC, CATTCTGTTG AATTCCTTCC;

Hmbs: CCTACCATACTACCTCCTGGCTTTAC, TTTGGGTGAAAGA CAACAGCAT;

Keratin 14 (Krt14): CCTCTGGCTCTCAGTCATCC, TGAGCAGCATGTA GCAGCTT;

Keratin 8 (Krt8): ATCGAGATCACCACCTACCG, CTGAAGCCAGGGC TAGTGAG;

CD11c: CTGGATAGCCTTTCTTCTGCTG, GCACACTGTGTCCGAA CTCA.

2.11. Statistical analysis

All statistical analyses were conducted on Graphpad Prism 5 software using Student's t-test; *P* values of less than 0.05 were considered significant.

3. Results

3.1. DC-SCRIPT$^{-/-}$ mice breed and grow abnormally

To understand the physiological functions of DC-SCRIPT, we successfully generated DC-SCRIPT$^{-/-}$ mice. Strikingly, DC-SCRIPT$^{-/-}$ mice could only be obtained by breeding female DC-SCRIPT$^{+/-}$ mice, not using DC-SCRIPT$^{-/-}$ female mice. Breeding of female DC-SCRIPT$^{+/-}$ mice with male DC-SCRIPT$^{+/-}$ mice (25 couples in total) for a one-year period yielded an offspring of 312 mice. Genotyping of the offspring revealed that the ratio of DC-SCRIPT$^{+/-}$ (N = 196) to DC-SCRIPT$^{+/+}$ (N = 97) pups was approximately 2 to1 in accordance with the theoretical Mendelian Ratio. In contrast, only 6% of the total offspring was DC-SCRIPT$^{-/-}$ (N = 19) representing only 8% (N = 13) of total female pups (N = 162) and 4% (N = 6) of total male pups (N = 150), respectively (Fig. 1A). An alternative breeding strategy using DC-SCRIPT$^{-/-}$ male mice and DC-SCRIPT$^{+/-}$ female mice yielded only one alive DC-SCRIPT$^{-/-}$ pup (data not shown). Analysis of the gender ratio amongst the entire 312 pups further showed that the ratio between females and males was around 1 to 1 in both DC-SCRIPT$^{+/+}$ (56 females and 41 males) and DC-SCRIPT$^{+/-}$ (93 females and 103 males) pups, while the ratio value exceeded 2 in DC-SCRIPT$^{-/-}$ offspring with 68% females (N = 13) and only 32% males (N = 6), respectively (Fig. 1B). Finally, we noted that DC-SCRIPT$^{-/-}$ offspring was smaller in size than age-matched wild-type littermates (DC-SCRIPT$^{+/+}$). Analysis of the body weight of mice revealed that DC-SCRIPT$^{-/-}$ mice were significantly lighter than their DC-SCRIPT$^{+/+}$ littermates, independent of age or gender (Fig. 1C and D).

3.2. DC-SCRIPT deficient mice show a delay in mammary morphogenesis in vivo

To better understand the role of DC-SCRIPT in mammary gland development, we focused on its role in mammary gland morphogenesis in DC-SCRIPT$^{-/-}$ mice and their littermate controls. Hereto, the architecture of mammary glands was investigated using whole-mount mammary glands (Fig. 2A). Compared to control 3 weeks old DC-SCRIPT$^{+/+}$ mice, rudimentary mammary epithelial ducts occupied smaller area and exhibited fewer amount of total branch points in DC-SCRIPT$^{-/-}$ mice (Fig. 2A, C). Of note: ductal length was not measured in these 3 weeks old mice since the rudimentary mammary epithelial ducts did not reach the lymph node and TEBs were not yet formed. Direct ductal tree visualization of 7 weeks old mice at puberty uncovered that mammary gland ductal elongation and bifurcation were significantly impaired in DC-SCRIPT$^{-/-}$ mice compared to wild-type littermates, which was confirmed by statistical analysis of ductal invasion area and distance (Fig. 2A, C). Consistently, mammary ducts from 7 weeks old DC-SCRIPT$^{-/-}$ mice had fewer TEBs and total number of branch points (Fig. 2B and C). Examination of ductal morphogenesis in virgin adult mice revealed the presence of tertiary branches and ductal elongation in both 18 weeks old DC-SCRIPT$^{+/+}$ and DC-SCRIPT$^{-/-}$ mice, whereas ductal branching morphogenesis was still repressed in DC-SCRIPT$^{-/-}$ mice (Fig. 2A, C). Interestingly, TEBs regressed completely in adult wild-type mice, leaving behind blunt-ended ductal termini, while in adult littermate DC-SCRIPT$^{-/-}$ mice TEBs were still detectable (Fig. 2B), indicative of delayed TEB regression.

3.3. DC-SCRIPT is expressed in basal and luminal mammary epithelium

Mammary gland ducts are known as bilayered structures composed of an inner luminal cell layer and an outside basal myoepithelial cell layer. Previously, DC-SCRIPT was shown to be expressed by cells of epithelial origin (Ansems et al., 2010a). To characterize the DC-SCRIPT expressing cells in mouse mammary epithelium more precisely, different mammary epithelial subpopulations were sorted based on CD49f and EpCAM

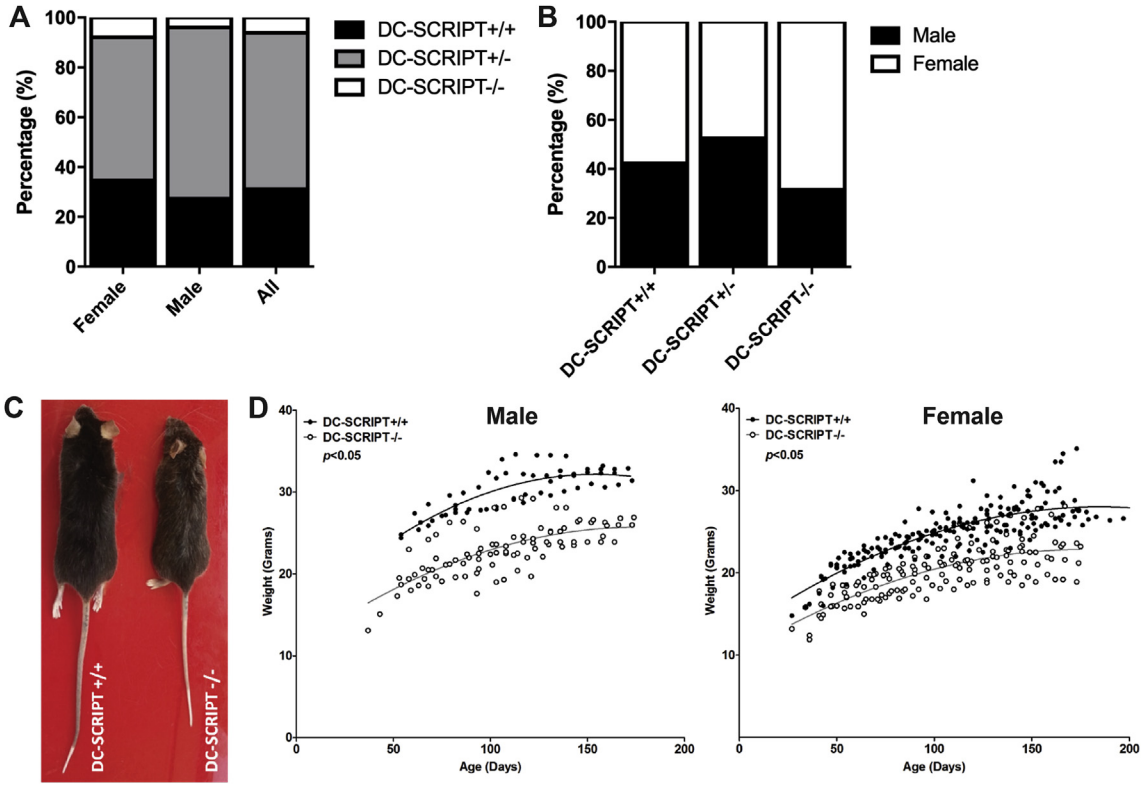

Fig. 1. DC-SCRIPT$^{-/-}$ mice breed and grow abnormally.
A) Percentage of DC-SCRIPT$^{+/+}$, DC-SCRIPT$^{+/-}$ and DC-SCRIPT$^{-/-}$ offspring of a heterozygous breeding strategy (312 pups in total). B) The percentage of male and female pups in DC-SCRIPT$^{+/+}$, DC-SCRIPT$^{+/-}$ and SCRIPT$^{-/-}$ mice (312 mice in total). C) Representative image showing of a DC-SCRIPT$^{+/+}$ and DC-SCRIPT$^{-/-}$ female mouse. D) Growth curve of male and female mice from DC-SCRIPT$^{+/+}$ and DC-SCRIPT$^{-/-}$ mice respectively (456 mice in total, Student's t-test, $p < 0.05$).

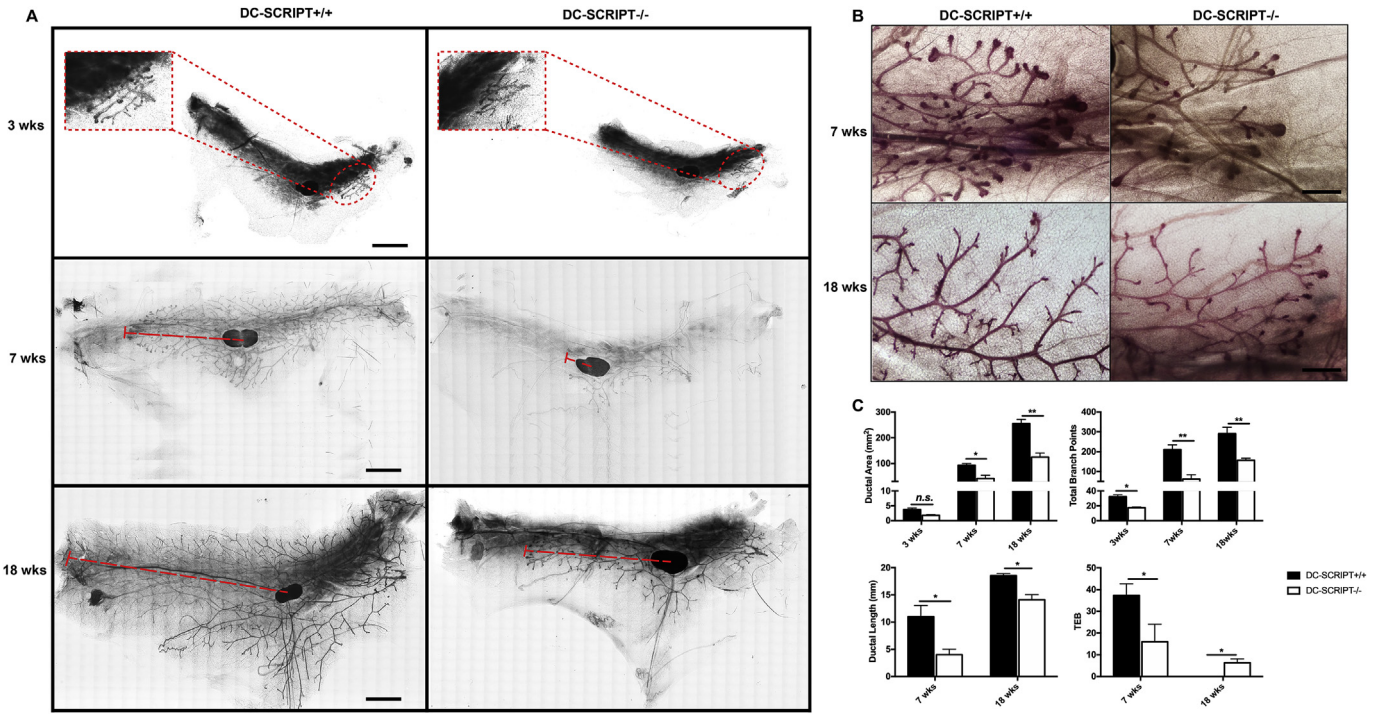

Fig. 2. Deletion of DC-SCRIPT delays mammary morphogenesis

A) Representative whole-mount staining of mammary glands from 3 weeks, 7 weeks and 18 weeks old DC-SCRIPT$^{+/+}$ and DC-SCRIPT$^{-/-}$ mice respectively, scale bar 3 mm. B) Representative whole-mount staining showing terminal morphology of mammary gland ducts from 7 to 18 weeks old DC-SCRIPT$^{+/+}$ and DC-SCRIPT$^{-/-}$ mice respectively, scale bar 1 mm. C) Quantification of ductal area, ductal length, total branch points and TEB number of mammary gland from DC-SCRIPT$^{+/+}$ and DC-SCRIPT$^{-/-}$ mice, Error bars represent mean ± S.E.M. (Data are collected from 3 mice of each group, Student's t-test, *p < 0.05, **p < 0.01, n.s, not significant).

expression by FACS (Fig. S2). Subsequent quantitative PCR analysis was performed on FACS-sorted basal and luminal epithelial cells of the mammary gland at puberty (7 weeks old) and virgin adult mice (18 weeks old). Interestingly, DC-SCRIPT mRNA expression was detected in both basal and luminal epithelium of the mammary gland in both developmental stages (Fig. 3A). RNA expression analysis of the basal and luminal specific epithelium marker keratin 14 and keratin 8, respectively, confirmed the purity of sorted mammary epithelial fractions. Importantly, expression of the DC marker CD11c was not detected in either of the sorted mammary epithelial samples, demonstrating that the epithelium was not contaminated with DCs that are known to express DC-SCRIPT mRNA (Fig. 3A). In concordance with the quantitative PCR data, double immunofluorescence staining for epithelial markers and DC-SCRIPT confirmed the presence of DC-SCRIPT protein in both keratin 14^{+} basal epithelium and keratin 8^{+} luminal epithelium located within the epithelial bilayer, which was detected in DC-SCRIPT$^{+/+}$ mice but not in DC-SCRIPT$^{-/-}$ littermate mice (Fig. 3B). Detectable nuclei staining of DC-SCRIPT protein was exhibited in a small number of mammary

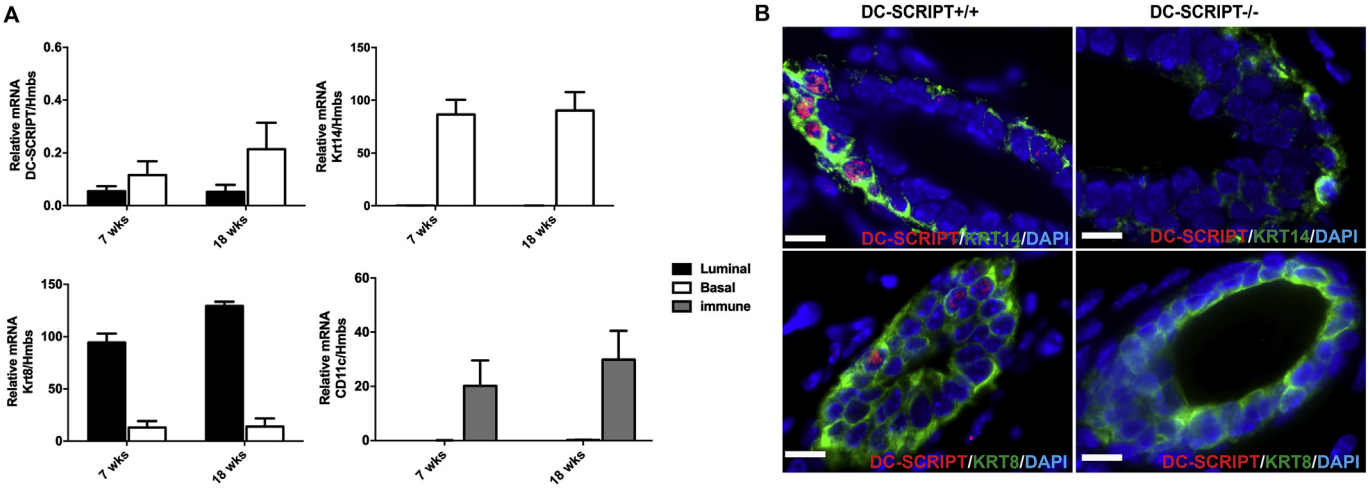

Fig. 3. DC-SCRIPT is expressed in mammary epithelium.

A) mRNA expression level of *DC-SCRIPT, Krt14, Krt8* and *CD11c* in basal and luminal epithelium is determined by quantitative RT-PCR on FACS sorted single cells from mammary gland of 7 and 18 weeks old C57BL/6 mice. Error bars represent mean ± S.E.M. (Data are collected from 6 mice of each group). B) Protein expression of DC-SCRIPT, KRT14 and KRT8 is detected by immunofluorescence staining in mammary gland paraffin section from 7 weeks old DC-SCRIPT$^{+/+}$ and DC-SCRIPT$^{-/-}$ mice respectively, scale bar 15 μm.

epithelial cells in DC-SCRIPT$^{+/+}$ mice (Fig. 3B).

3.4. DC-SCRIPT deficiency changes mammary tissue stoichiometry in adult mice

Mammary gland morphogenesis depends on homeostasis between the different mammary epithelial subsets (Visvader and Stingl, 2014; Oakes et al., 2014a). To determine the effect of DC-SCRIPT deficiency on epithelial homeostasis within the mammary gland, epithelial subpopulations were enumerated in mature virgin adult glands (18 weeks) by flow cytometry using the markers EpCAM and CD49f (Fig. S2, Fig. 4A and Fig. S3). Our data show large variation in the luminal (EpCAM^{high}CD49f^{low}) to basal cells (EpCAM^{low}CD49f^{high}) ratio (L/B) between different mice of similar age within the same group. We did, however, observe a mean L/B ratio of 0.67 in DC-SCRIPT$^{+/+}$ mice, while littermate DC-SCRIPT$^{-/-}$ mice show a mean L/B ratio of 0.98 (Fig. 4A). Although this difference did not reach significance, these data may suggest that loss of DC-SCRIPT tends to change epithelium homeostasis. Of note: characterizing the basal and luminal population based on the epithelial cell markers EpCAM and CD49f was highly comparable to using the markers CD24 and CD49f (Fig. S3). Subsequently, precursor and mature cell subsets within the heterogeneous luminal subpopulation were examined using the previously reported cell markers Sca1 and CD49b (Giraddi et al., 2015). The ratio of luminal precursor cells (EpCAM^{high}CD49f^{low}Sca1$^{+/-}$CD49b^{+}) to mature luminal (EpCAM^{high}CD49f^{low}Sca1^{+}CD49b^{-}) cells was dramatically decreased in DC-SCRIPT$^{-/-}$ mice compared to DC-SCRIPT$^{+/+}$ mice (Fig. 4B). These data thus confirm that DC-SCRIPT has a significant impact on mammary epithelium homeostasis, in particular on the luminal subpopulation within the mammary gland.

3.5. DC-SCRIPT deletion delays mammary gland organoid branching in vitro

To study the impact of DC-SCRIPT on the kinetics of mammary branching morphogenesis in more detail, we made use of a 3D mammary gland organoid model. *Ex vivo* 3D organoid cultures showed that mammary organoids developed and were able to branch using cells derived from both DC-SCRIPT$^{+/+}$ and DC-SCRIPT$^{-/-}$ mice (Fig. 5A). Interestingly, the phenotype of organoids was more cystic-like with limited branching in DC-SCRIPT$^{-/-}$ as compared to the more compact branched phenotype in DC-SCRIPT$^{+/+}$ on day 4 (Fig. 5A). However, these differences gradually reduced as both groups developed towards a more fully branched compact phenotype on day 6 (Fig. S4). To further quantify the status of mammary gland branching morphogenesis, organoids were categorized into different grades according to their branching status

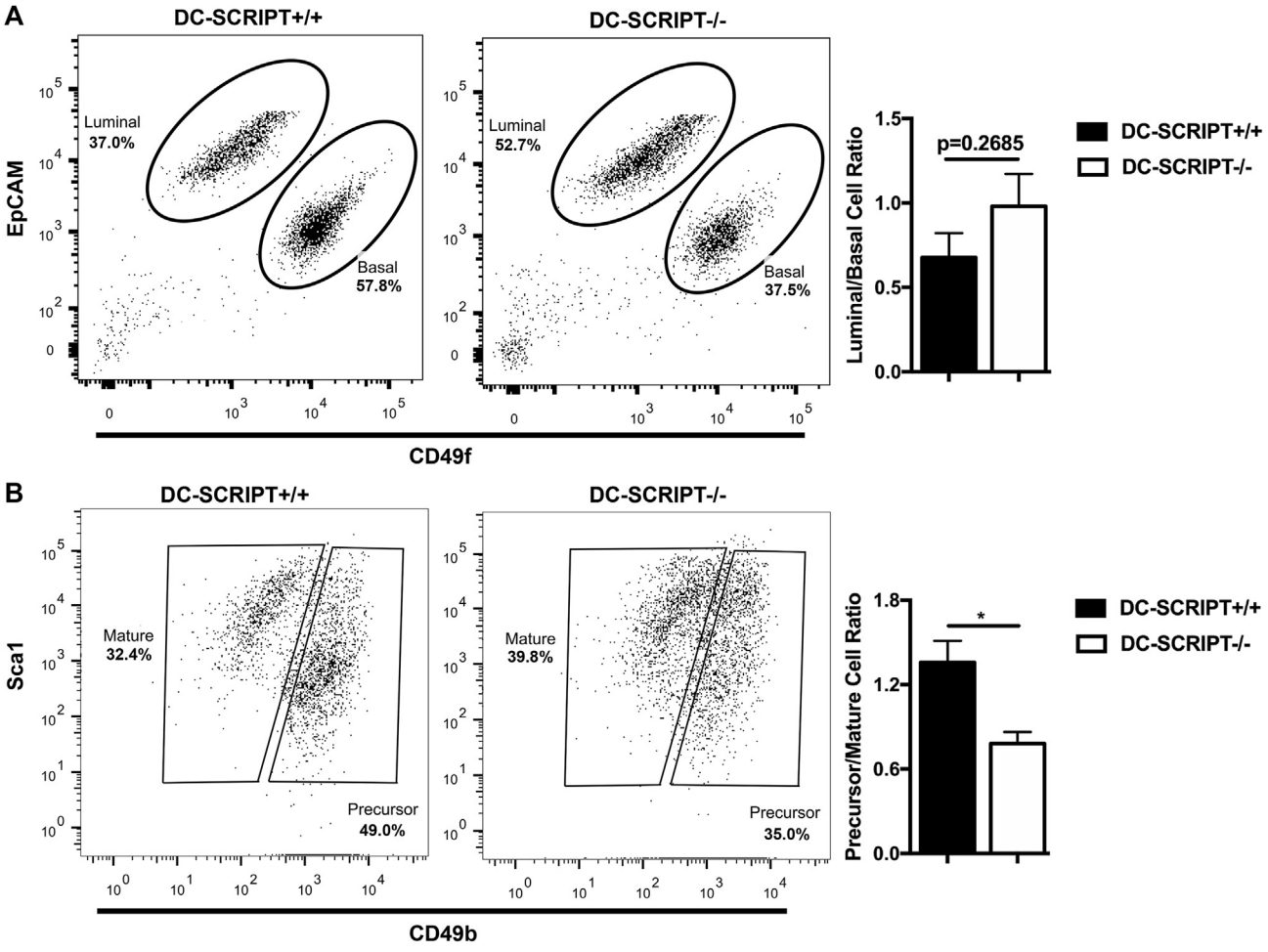

Fig. 4. Deficiency of DC-SCRIPT changes mammary tissue stoichiometry in adult mice

A) Representative FACS analysis of luminal (EpCAM^{high}CD49f^{low}) and basal (EpCAM^{low}CD49f^{high}) subpopulations from the mammary gland of 18 weeks old DC-SCRIPT$^{+/+}$ and DC-SCRIPT$^{-/-}$ mice. Bar graph shows the quantification of the ratio of luminal subpopulations to basal subpopulations. Error bars represent mean ± S.E.M. (Data are collected from at least 5 mice per group, Student's t-test). B) Representative FACS analysis of mature luminal subset (Sca1^{+}CD49b^{-}) and luminal precursor subset (Sca1^{+}CD49b^{+} and Sca1^{-}CD49b^{+}) in mammary luminal subpopulations from 18 weeks old DC-SCRIPT$^{+/+}$ and DC-SCRIPT$^{-/-}$ mice. Bar graph shows the quantification of the ratio of luminal precursor subset to mature luminal subset. Error bars represent mean ± S.E.M. (Data are collected from 4 mice per group, Student's t-test, *$p < 0.05$).

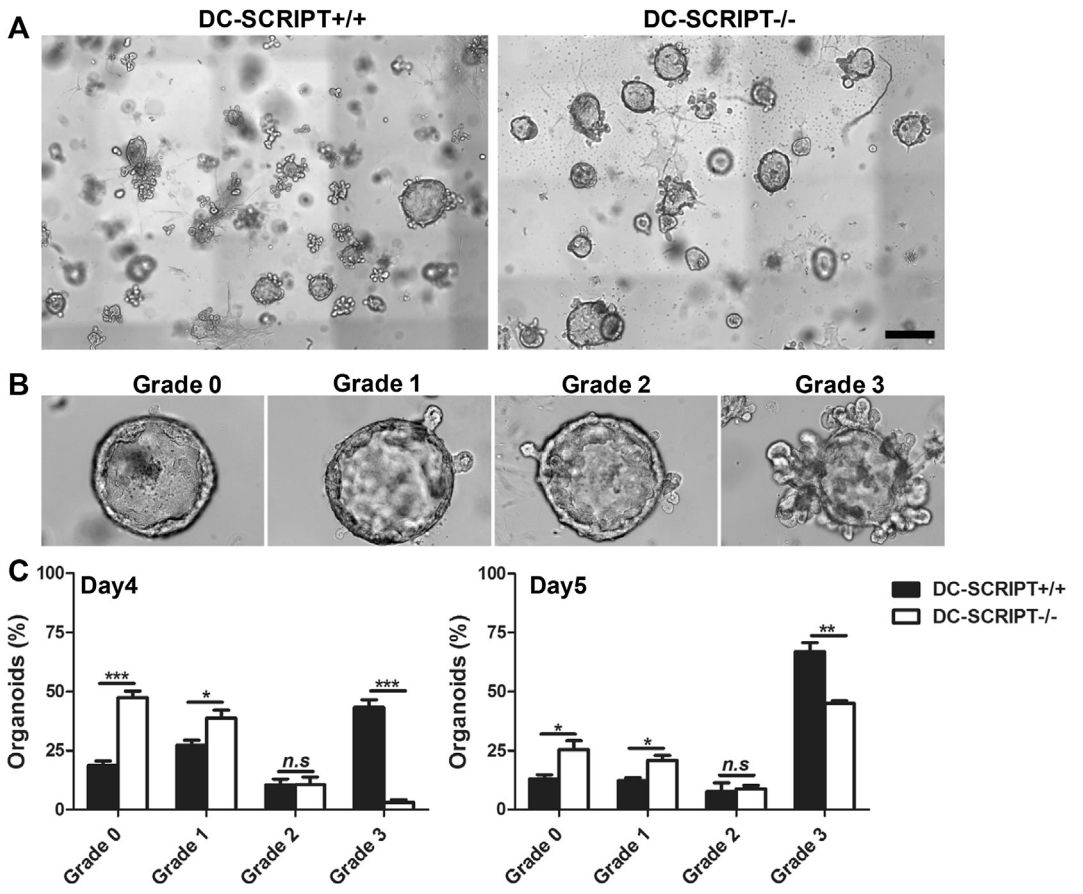

Fig. 5. DC-SCRIPT deletion delays mammary gland organoids branching *in vitro*

A) Representative image of *in vitro* cultured mammary gland organoids on day 4 derived from 18 weeks old DC-SCRIPT$^{+/+}$ and DC-SCRIPT$^{-/-}$ mice, scale bar 300 μm. B) Representative images for grading of branching in organoid. Grade 0, no branches; Grade 1, 1–3 branches; Grade 2, 4–6 branches; Grade 3, more than 6 branches. C) Quantification of mammary gland organoid branching *in vitro* from DC-SCRIPT$^{+/+}$ and DC-SCRIPT$^{-/-}$ mice on day 4 and 5, respectively. Error bars represent mean ± S.E.M. (Data are collected from 4 mice per group, Student's t-test, *p < 0.05, **p < 0.01, ***p < 0.001, *n.s,* not significant).

(Fig. 5B). Strikingly, compared to organoids from DC-SCRIPT$^{+/+}$, organoids derived from DC-SCRIPT$^{-/-}$ mice showed a remarkably higher percentage of non-branched and partially branched organoids (Grade 0, 1 and 2) and a lower percentage of fully branched organoids (Grade 3) on days 4 and 5 (Fig. 5C). These data confirmed that branching morphogenesis in mammary gland organoids at early time points was significantly delayed in the absence of DC-SCRIPT. Subsequent quantification of branching status at day 6 showed that both DC-SCRIPT$^{+/+}$ and DC-SCRIPT$^{-/-}$ organoids continued to branch, thereby dramatically increasing the percentage of fully branched organoids (Fig. S4). Altogether, our *ex vivo* findings demonstrate that DC-SCRIPT deficiency delayed mammary organoid branching morphogenesis thereby reproducing the findings in DC-SCRIPT deficient mice.

4. Discussion

The early loss of DC-SCRIPT expression during malignant transformation of ductal mammary epithelial cells led us to investigate the role of DC-SCRIPT in normal mammary gland development. Our data show that DC-SCRIPT is expressed in both basal and luminal epithelium and can affect epithelial cell homeostasis within the mammary gland. Moreover, our data in DC-SCRIPT deficient mice show that DC-SCRIPT plays an important role in controlling mammary gland morphogenesis, affecting mammary gland elongation and bifurcation. Using a 3D mammary gland organoid culture system, we demonstrate that DC-SCRIPT deletion delays but does not prevent branching of mammary gland organoids *in vitro*.

Our previous studies have shown that DC-SCRIPT is a multifunctional transcription factor playing a significant role in breast cancer cell proliferation as well as cell cycle progression (Ansems et al., 2010a, 2015). Indeed, the presence of the transcription factor DC-SCRIPT is a favorable prognostic factor for ER positive breast cancer patients (Ansems et al., 2010a; Sieuwerts et al., 2010). The murine ortholog of DC-SCRIPT is highly conserved and contains >80% homology to the human DC-SCRIPT protein (Triantis et al., 2006b). To elucidate the physiological function of DC-SCRIPT, analysis of DC-SCRIPT deficient mice could be rewarding. In our current study we have for the first time used DC-SCRIPT$^{-/-}$ mice to evaluate the function of DC-SCRIPT. These studies were hampered by the observation that deletion of DC-SCRIPT not only impaired the growth of the mice, but simultaneously affected the reproductive capacity of female mice. The impact of DC-SCRIPT on the reproductive capacity of mice is in line with DC-SCRIPT being a multi-functional factor involved in various regulatory processes, including the regulation of the estrogen and progesterone hormone NRs (Ansems et al., 2010b). Unfortunately, our preliminary data on selected hormones (progesterone, testosterone) tested in the circulation on a limited number of available mice revealed huge mouse-mouse variations in hormone levels and did not reveal significant differences in hormone levels between adult mice of different genotypes. In addition, currently unknown additional functions of DC-SCRIPT beyond our previous studies may be involved as well, and are the topic for our further investigations. Furthermore, in the very limited number of DC-SCRIPT$^{-/-}$ mice analyzed so far, we did not discern an increase in tumorigenesis although this may require aging of the mice.

Given the relationship between breast tumorigenesis and mammary gland development (Visvader, 2009; Oakes et al., 2014b), we first investigated the role of DC-SCRIPT in mammary gland development. During postnatal mammary gland development remarkable structural alterations occur that are controlled by numerous regulators (Hennighausen and Robinson, 2005; Sternlicht, 2006; Strange et al., 2007). Histological examination of whole-mounted mammary glands uncovered that DC-SCRIPT$^{-/-}$ mice exhibit impaired ductal morphogenesis, implicating DC-SCRIPT as a novel regulator in mammary gland development. Most strikingly, in the early developmental stage, underdevelopment of the embryonically established rudimentary mammary tree was already detected in DC-SCRIPT$^{-/-}$ mice. These data are in line with the major effects on the branching morphogenesis during puberty in DC-SCRIPT$^{-/-}$ mice. The difference in mammary morphogenesis between DC-SCRIPT$^{-/-}$ and littermate wild-type mice is gradually disappearing with increasing age. These data imply that DC-SCRIPT deficiency delays but does not block mammary gland development. TEBs are unique structures present in puberty and crucial for driving mammary duct elongation and bifurcation (Morris and Stein, 2017). DC-SCRIPT deficiency leads to fewer TEBs and total number of branch points in 7 weeks old mice. The importance of DC-SCRIPT in TEBs is further supported by the finding that also in adult DC-SCRIPT$^{-/-}$ mice the regression of TEBs is postponed. Due to the impaired reproductive capability of female DC-SCRIPT$^{-/-}$ mice, its role in mammary gland morphogenesis during pregnancy could not be evaluated in the current study. Conditional or cell type-specific DC-SCRIPT$^{-/-}$ mouse models may be required to study the effect of DC-SCRIPT in mammary gland morphogenesis during different developmental stages.

A 3D culture model of organoids is a powerful tool to study mammary gland morphogenesis *in vitro* as it mimics the mammary gland structurally and functionally (Kretzschmar and Clevers, 2016; Jamieson et al., 2017). In addition, 3D mammary gland organoid culture enables evaluation of the impact of specific factors in mammary gland morphogenesis in a defined culture environment (Nguyen-Ngoc et al., 2015; Furuta and Bissell, 2016). Mammary gland organoids cultured from DC-SCRIPT$^{-/-}$ mice and littermate wild-type mice both successfully grew and branched in the 3D organoid culture system, demonstrating that mammary gland morphogenesis *in vitro* can occur independent of DC-SCRIPT. However, during early stage of organoid branching morphogenesis, loss of DC-SCRIPT dramatically delayed branching of organoids. These data imply that DC-SCRIPT expression is important for organoid branching at the early stages and are consistent with our *in vivo* data showing that DC-SCRIPT deficiency significantly delays but does not terminally diminish mammary gland development. Besides affecting organoids branching, we cannot yet exclude that DC-SCRIPT deletion has some additional, more subtle effects on organoid morphogenesis. In this context we have noted a slight difference in cystic-like and compact branched phenotypes of organoids derived from DC-SCRIPT$^{+/+}$ and DC-SCRIPT$^{-/-}$ mice *in vitro* that requires further studies.

The epithelium of mammary ductal tree is organized as a bilayer composed of inner luminal epithelium and outer basal epithelium (Smith, 2012). We therefore investigated the expression of DC-SCRIPT mRNA in these two major epithelial populations. Interestingly, DC-SCRIPT mRNA is detected in both the basal and the luminal epithelial subpopulation. In line with relatively low DC-SCRIPT mRNA expression level detected in both epithelial cell populations, we noted that only few cells express detectable DC-SCRIPT protein levels. This heterogeneity of protein expression is known to exist within the luminal and basal subpopulation (Oakes et al., 2014b; Pal et al., 2017).

Previously, in wild type mice different L/B ratios have been reported (Shehata et al., 2012; Smalley et al., 2012) and they even seem to dynamically change during growth (Dong et al., 2016). Interestingly, we also found a large variation in L/B ratio between mice and our data pointed toward an increased L/B ratio in the absence of DC-SCRIPT. This observation is consistent with delayed mammary gland development in DC-SCRIPT$^{-/-}$ mice, as a decrease in the ratio between luminal and basal mammary epithelium subpopulations has previously been related to aging of mice (Dong et al., 2016). Together with the finding that DC-SCRIPT deletion decreases the ratio of precursor to mature cells within luminal population, our data suggest that DC-SCRIPT expression is necessary to maintain a proper hierarchical relationship between the distinct subpopulations within the mammary epithelium. Characterizing the impact of DC-SCRIPT expression on mature and progenitor basal subpopulations will also be interesting, but is much more complex as markers for these subpopulations still need to be defined. In future follow-up studies it will be important to define which specific cell subsets express DC-SCRIPT within the basal and luminal epithelium. The 3D *in vitro* organoid model system, in combination with the DC-SCRIPT deficient mice should allow to elucidate this and the molecular mechanism by which DC-SCRIPT regulates mammary gland (organoids) morphogenesis.

5. Conclusion

In conclusion, the data presented in this study indicate that DC-SCRIPT represents a novel regulator of mammary gland branching and development. Studying the role of DC-SCRIPT in mammary gland morphogenesis will be important for understanding its role in breast cancer tumorigenesis.

Ethics approval

All protocols for generation of DC-SCRIPT knockout mice were carried out in accordance with and approved by the Institutional Animal Care and Use Committee at Washington University in St. Louis, MO, United State. All mice were bred and housed at the Animal Research Facility of the Radboud University Medical Center. All animal experiments were documented and approved by the Animal Experimental Committee of the Radboud University Medical Center and were performed in accordance with regulatory standards of the Animal Experimental Committee.

Availability of data and materials

All data generated or analyzed during this study are included in this published article and its supplementary material.

Conflicts of interest

The authors declare no conflict of interest.

Funding

This work was supported by the China Scholarship Council (Project No. 201406990002); Dutch Cancer Society (Project No. BUIT, 2012-5347); the Netherlands Organisation for Scientific Research (Project No. 016.156.093).

Authors' contributions

CT and RB carried out the experimental work and collected the data; CT analyzed the data and prepared the figures; AMG, MWGL, NTK assisted in the experimental work. CT, MA and GJA participated in design and coordination of the project, and drafted the manuscript; SG and MC generated and provided the DC-SCRIPT$^{-/-}$ mice. All authors read and approved the final manuscript.

Acknowledgement

CT was supported by the China Scholarship Council (Project No.201406990002). MA is a recipient of a long-term fellowship (BUIT 2012–5347) from the Dutch Cancer Society and a NWO-Veni fellowship

(016.156.093) of the Netherlands Organization for Scientific Research (NWO-Veni).

List of abbreviations

DC-SCRIPT	Dendritic cell specific transcript
DCs	Dendritic cells
ER	Estrogen receptor
NRs	Nuclear receptors
TEBs	Terminal end buds
MaSCs	Mammary stem cells
DUSP4	Dual specificity phosphatase 4
MAPK	Mitogen-activated protein kinases
RT-PCR	Reverse transcription-polymerase chain reaction

Appendix A. Supplementary data

Supplementary data to this article can be found online at https://doi.org/10.1016/j.ydbio.2019.06.023.

References

Ansems, M., Hontelez, S., Looman, M.W., Karthaus, N., Bult, P., Bonenkamp, J.J., Jansen, J.H., Sweep, F.C., Span, P.N., Adema, G.J., SCRIPT, D.C.-, 2010. Nuclear receptor modulation and prognostic significance in primary breast cancer. J. Natl. Cancer Inst. 102 (1), 54–68.

Ansems, M., Hontelez, S., Karthaus, N., Span, P.N., Adema, G.J., 2010. Crosstalk and DC-SCRIPT: expanding nuclear receptor modulation. Biochim. Biophys. Acta 1806 (2), 193–199.

Ansems, M., Karthaus, N., Hontelez, S., Aalders, T., Looman, M.W., Verhaegh, G.W., Schalken, J.A., Adema, G.J., SCRIPT, D.C.-, 2012. AR and VDR regulator lost upon transformation of prostate epithelial cells. Prostate 72 (16), 1708–1717.

Ansems, M., Sondergaard, J.N., Sieuwerts, A.M., Looman, M.W., Smid, M., de Graaf, A.M., de Weerd, V., Zuidscherwoude, M., Foekens, J.A., Martens, J.W., et al., 2015. DC-SCRIPT is a novel regulator of the tumor suppressor gene CDKN2B and induces cell cycle arrest in ERalpha-positive breast cancer cells. Breast Canc. Res. Treat. 149 (3), 693–703.

Asselin-Labat, M.L., Vaillant, F., Sheridan, J.M., Pal, B., Wu, D., Simpson, E.R., Yasuda, H., Smyth, G.K., Martin, T.J., Lindeman, G.J., et al., 2010. Control of mammary stem cell function by steroid hormone signalling. Nature 465 (7299), 798–802.

Ball, S.M., 1998. The development of the terminal end bud in the prepubertal-pubertal mouse mammary gland. Anat. Rec. 250 (4), 459–464.

Brisken, C., 2002. Hormonal control of alveolar development and its implications for breast carcinogenesis. J. Mammary Gland Biol. Neoplasia 7 (1), 39–48.

Brisken, C., O'Malley, B., 2010. Hormone action in the mammary gland. Cold Spring Harb. Perspect. Biol. 2 (12), a003178.

Dong, Q., Gao, H., Shi, Y., Zhang, F., Gu, X., Wu, A., Wang, D., Chen, Y., Bandyopadhyay, A., Yeh, I.T., et al., 2016. Aging is associated with an expansion of CD49f(hi) mammary stem cells that show a decline in function and increased transformation potential. Aging (Albany NY) 8 (11), 2754–2776.

Fu, N.Y., Rios, A.C., Pal, B., Law, C.W., Jamieson, P., Liu, R., Vaillant, F., Jackling, F., Liu, K.H., Smyth, G.K., et al., 2017. Identification of quiescent and spatially restricted mammary stem cells that are hormone responsive. Nat. Cell Biol. 19 (3), 164–176.

Furuta, S., Bissell, M.J., 2016. Pathways involved in formation of mammary organoid architecture have keys to understanding drug resistance and to discovery of druggable targets. Cold Spring Harbor Symp. Quant. Biol. 81, 207–217.

Giraddi, R.R., Shehata, M., Gallardo, M., Blasco, M.A., Simons, B.D., Stingl, J., 2015. Stem and progenitor cell division kinetics during postnatal mouse mammary gland development. Nat. Commun. 6, 8487.

Hennighausen, L., Robinson, G.W., 2005. Information networks in the mammary gland. Nat. Rev. Mol. Cell Biol. 6 (9), 715–725.

Hontelez, S., Karthaus, N., Looman, M.W., Ansems, M., Adema, G.J., 2013. DC-SCRIPT regulates glucocorticoid receptor function and expression of its target GILZ in dendritic cells. J. Immunol. 190 (7), 3172–3179.

Jamieson, P.R., Dekkers, J.F., Rios, A.C., Fu, N.Y., Lindeman, G.J., Visvader, J.E., 2017. Derivation of a robust mouse mammary organoid system for studying tissue dynamics. Development 144 (6), 1065–1071.

Joshi, P.A., Jackson, H.W., Beristain, A.G., Di Grappa, M.A., Mote, P.A., Clarke, C.L., Stingl, J., Waterhouse, P.D., Khokha, R., 2010. Progesterone induces adult mammary stem cell expansion. Nature 465 (7299), 803–807.

Kretzschmar, K., Clevers, H., 2016. Organoids: modeling development and the stem cell niche in a dish. Dev. Cell 38 (6), 590–600.

Livak, K.J., Schmittgen, T.D., 2001. Analysis of relative gene expression data using real-time quantitative PCR and the 2(-Delta Delta C(T)) Method. Methods 25 (4), 402–408.

Lloyd-Lewis, B., Harris, O.B., Watson, C.J., Davis, F.M., 2017. Mammary stem cells: premise, properties, and perspectives. Trends Cell Biol. 27 (8), 556–567.

Macias, H., Hinck, L., 2012. Mammary gland development. Wiley Interdiscip. Rev. Dev. Biol. 1 (4), 533–557.

Morris, J.S., Stein, T., 2017. Pubertal ductal morphogenesis: isolation and transcriptome analysis of the terminal end bud. Methods Mol. Biol. 1501, 131–148.

Nguyen-Ngoc, K.V., Shamir, E.R., Huebner, R.J., Beck, J.N., Cheung, K.J., Ewald, A.J., 2015. 3D culture assays of murine mammary branching morphogenesis and epithelial invasion. Methods Mol. Biol. 1189, 135–162.

Oakes, S.R., Gallego-Ortega, D., Ormandy, C.J., 2014. The mammary cellular hierarchy and breast cancer. Cell. Mol. Life Sci. 71 (22), 4301–4324.

Oakes, S.R., Gallego-Ortega, D., Ormandy, C.J., 2014. The mammary cellular hierarchy and breast cancer. Cell. Mol. Life Sci. 71 (22), 4301–4324.

Paine, I.S., Lewis, M.T., 2017. The terminal end bud: the little engine that could. J. Mammary Gland Biol. Neoplasia 22 (2), 93–108.

Pal, B., Chen, Y., Vaillant, F., Jamieson, P., Gordon, L., Rios, A.C., Wilcox, S., Fu, N., Liu, K.H., Jackling, F.C., et al., 2017. Construction of developmental lineage relationships in the mouse mammary gland by single-cell RNA profiling. Nat. Commun. 8 (1), 1627.

Plaks, V., Boldajipour, B., Linnemann, J.R., Nguyen, N.H., Kersten, K., Wolf, Y., Casbon, A.J., Kong, N., van den Bijgaart, R.J., Sheppard, D., et al., 2015. Adaptive immune regulation of mammary postnatal organogenesis. Dev. Cell 34 (5), 493–504.

Prater, M.D., Petit, V., Alasdair Russell, I., Giraddi, R.R., Shehata, M., Menon, S., Schulte, R., Kalajzic, I., Rath, N., Olson, M.F., et al., 2014. Mammary stem cells have myoepithelial cell properties. Nat. Cell Biol. 16 (10), 942-950, 941-947.

Riegert, P., Gilfillan, S., 1999. A conserved sequence block in the murine and human TCR J alpha region: assessment of regulatory function in vivo. J. Immunol. 162 (6), 3471–3480.

Schwenk, F., Baron, U., Rajewsky, K., 1995. A cre-transgenic mouse strain for the ubiquitous deletion of loxP-flanked gene segments including deletion in germ cells. Nucleic Acids Res. 23 (24), 5080–5081.

Shehata, M., Teschendorff, A., Sharp, G., Novcic, N., Russell, I.A., Avril, S., Prater, M., Eirew, P., Caldas, C., Watson, C.J., et al., 2012. Phenotypic and functional characterisation of the luminal cell hierarchy of the mammary gland. Breast Cancer Res. 14 (5), R134.

Sieuwerts, A.M., Ansems, M., Look, M.P., Span, P.N., de Weerd, V., van Galen, A., Foekens, J.A., Adema, G.J., Martens, J.W., 2010. Clinical significance of the nuclear receptor co-regulator DC-SCRIPT in breast cancer: an independent retrospective validation study. Breast Cancer Res. 12 (6), R103.

Smalley, M.J., Kendrick, H., Sheridan, J.M., Regan, J.L., Prater, M.D., Lindeman, G.J., Watson, C.J., Visvader, J.E., Stingl, J., 2012. Isolation of mouse mammary epithelial subpopulations: a comparison of leading methods. J. Mammary Gland Biol. Neoplasia 17 (2), 91–97.

Smith, G.H., 2012. Biology of mammary gland development. Semin. Cell Dev. Biol. 23 (5), 546.

Sondergaard, J.N., Poghosyan, S., Hontelez, S., Louche, P., Looman, M.W., Ansems, M., Adema, G.J., 2015. DC-SCRIPT regulates IL-10 production in human dendritic cells by modulating NF-kappaBp65 activation. J. Immunol. 195 (4), 1498–1505.

Sondergaard, J.N., van Heeringen, S.J., Looman, M.W.G., Tang, C., Triantis, V., Louche, P., Janssen-Megens, E.M., Sieuwerts, A.M., Martens, J.W.M., Logie, C., et al., 2018. Dendritic cells actively limit interleukin-10 production under inflammatory conditions via DC-SCRIPT and dual-specificity phosphatase 4. Front. Immunol. 9, 1420.

Sternlicht, M.D., 2006. Key stages in mammary gland development: the cues that regulate ductal branching morphogenesis. Breast Cancer Res. 8 (1), 201.

Strange, R., Westerlind, K.C., Ziemiecki, A., Andres, A.C., 2007. Proliferation and apoptosis in mammary epithelium during the rat oestrous cycle. Acta Physiol. 190 (2), 137–149.

Trejo, C.L., Luna, G., Dravis, C., Spike, B.T., Wahl, G.M., 2017. Lgr5 is a marker for fetal mammary stem cells, but is not essential for stem cell activity or tumorigenesis. NPJ breast cancer 3, 16.

Triantis, V., Trancikova, D.E., Looman, M.W., Hartgers, F.C., Janssen, R.A., Adema, G.J., 2006. Identification and characterization of DC-SCRIPT, a novel dendritic cell-expressed member of the zinc finger family of transcriptional regulators. J. Immunol. 176 (2), 1081–1089.

Triantis, V., Moulin, V., Looman, M.W., Hartgers, F.C., Janssen, R.A., Adema, G.J., 2006. Molecular characterization of the murine homologue of the DC-derived protein DC-SCRIPT. J. Leukoc. Biol. 79 (5), 1083–1091.

Visvader, J.E., 2009. Keeping abreast of the mammary epithelial hierarchy and breast tumorigenesis. Genes Dev. 23 (22), 2563–2577.

Visvader, J.E., Stingl, J., 2014. Mammary stem cells and the differentiation hierarchy: current status and perspectives. Genes Dev. 28 (11), 1143–1158.

Wang, D., Cai, C., Dong, X., Yu, Q.C., Zhang, X.O., Yang, L., Zeng, Y.A., 2015. Identification of multipotent mammary stem cells by protein C receptor expression. Nature 517 (7532), 81–84.